JACS
JOURNAL OF THE AMERICAN CHEMICAL SOCIETY
Article
pubs.acs.org/JACS

Three-Coordinate Nickel Carbene Complexes and Their One-Electron Oxidation Products

Vlad M. Iluc* and Gregory L. Hillhouse

Gordon Center for Integrative Science, Department of Chemistry, The University of Chicago, Chicago, Illinois 60637, United States

Supporting Information

ABSTRACT: The synthesis and characterization of two new carbene complexes, (dtbpe)Ni=CH(dmp) (**1**; dtbpe = 1,2-bis(di-*tert*-butylphosphino)ethane; dmp = 2,6-dimesitylphenyl) and (dippn)Ni=CH(dmp) (**2**; dippn = 1,8-bis(di-*iso*-propylphosphino)naphthalene), are described. Complexes **1** and **2** were isolated by photolysis of the corresponding side-bound diazoalkane complexes, exemplified by (dtbpe)Ni{η^2-N_2CH(dmp)} (**3**). The carbene complexes feature Ni−C distances that are short and Ni−C−C angles at the carbene carbon that are intermediate between 120° and 180° (155.7(3)° and 152.3(3)°, respectively). The difference between the two carbenes became obvious when their reactivity toward 1-electron oxidizing agents was studied: the oxidation of **1** led to an internal rearrangement and the formation of a nickel(I) alkyl [{κ^2-P,C-di-*tert*-butylphosphino-di-*tert*-butyl-PCH(dmp)ethane}Ni][BAr^F_4] (**4**), while the oxidation of **2** allowed the isolation of an unrearranged product, formulated as the cationic nickel(III) carbene complex[(dippn)Ni=CH(dmp)][BAr^F_4] (**6**). Both oxidations are chemically reversible and the respective reductions lead to the neutral carbene complexes, **1** and **2**.

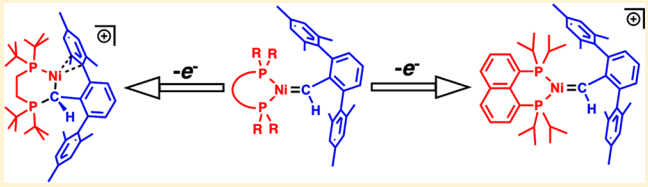

INTRODUCTION

Low-coordinate, late-transition metal complexes are important targets in synthetic organometallic chemistry because these species show unique reactivity in small molecule activation.[1,2] Although terminal nickel imides are well established, there are few reported examples of nickel carbenes: (dtbpe)Ni=CPh_2 (dtbpe = 1,2-bis(di-*tert*-butylphosphino)ethane)[3] and the supporting ligand-based carbene ($PC_{carbene}P$)$NiPR_3$ ($PC_{carbene}P$ = *o*-$^i Pr_2$P-C_6H_4-$C_{carbene}$-C_6H_4-P$^i Pr_2$-*o*).[4] This situation extends to other late-transition metals as well, with only a handful of non-Fisher carbenes being known.[5−8]

The previously isolated nickel carbene (dtbpe)Ni=CPh_2[3] took advantage of the special characteristics of the dtbpe ligand, which increases the steric congestion around the metal center and supports multiple bonds between nickel and π donors.[3,9,10] We became interested in exploring whether a species with a noninteger Ni−C bond order in the (dtbpe)Ni=CPh_2 manifold was accessible. Herein, we report the synthesis of two new nickel(II) complexes, (dtbpe)Ni=CH(dmp) (**1**, dmp = 2,6-dimesitylphenyl) and (dippn)Ni=CH(dmp) (**2**, dippn = 1,8-bis(di-*iso*-propylphosphino)naphthalene), which feature hydrogen and a bulky aryl group as substituents at the carbene carbon. The ancillary ligand dippn is introduced to engender rigidity and to prevent the dissociation of a phosphine donor, a process observed for dtbpe in some cases.[11] The one-electron oxidations of **1** and **2** are also discussed. The oxidation of **1** led to an internal rearrangement and the formation of a nickel(I) alkyl [{κ^2-P,C-di-*tert*-butylphosphino-di-*tert*-butyl-PCH(dmp)-ethane}Ni][BAr^F_4] (**4**). The oxidation of **2** allowed the isolation of an unrearranged product, formulated as the cationic nickel(III) carbene complex [(dippn)Ni=CH(dmp)][BAr^F_4] (**6**). These oxidations are chemically reversible and the respective reductions lead to the neutral carbene complexes **1** and **2**.

RESULTS AND DISCUSSION

The reaction of the Ni(0)-benzene adduct {(dtbpe)Ni}$_2$(μ-C_6H_6) with (dmp)CHN_2[12] (Scheme 1) led to the formation of the side-bound diazo complex (dtbpe)Ni{η^2-N_2CH(dmp)} (**3**). The reaction took place rapidly at room temperature in hexanes or pentanes, and the isolation of **3** was facilitated by its low solubility in hydrocarbon solvents. Its IR spectrum showed a

Scheme 1. Formation of (dtbpe)Ni=CH(dmp) (1)

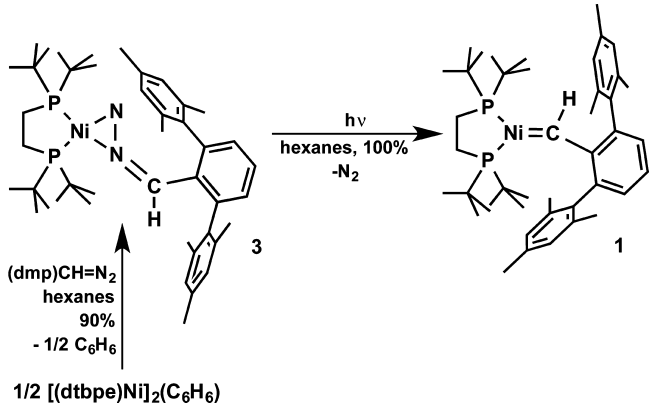

Received: March 1, 2014
Published: April 9, 2014

   dx.doi.org/10.1021/ja501900j | J. Am. Chem. Soc. 2014, 136, 6479−6488

characteristic $\nu_{C=N}$ at 2058 cm^{-1} (cf. 2052 cm^{-1} in (dmp)-CH=N_2) and $\nu_{N=N}$ at 1518 cm^{-1} (cf. 1437 cm^{-1} in (dmp)CH=N_2).[12] The NMR spectra of **3** are consistent with an unsymmetrical, planar geometry around the metal center, with chemically nonequivalent environments for the two phosphorus nuclei (δ 91.9, 88.9; J_{PP} = 63.2 Hz). In the ^{1}H NMR spectrum, the resonance for the unique hydrogen of the diazo ligand was found as a doublet at 5.36 ppm, coupled to one phosphine ($^4J_{HP}$ = 6 Hz) and shifted by more than 1 ppm from the resonance for free (dmp)CH=N_2 (δ = 4.04).

The solid-state molecular structure of **3**, determined by single-crystal X-ray diffraction (Figure 1), features a planar

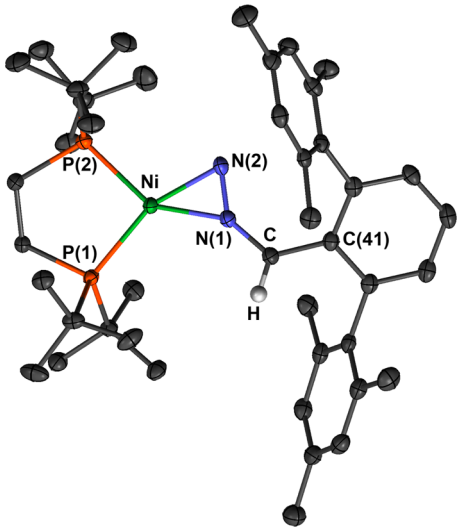

Figure 1. Thermal-ellipsoid (50% probability) representation of (dtbpe)Ni{η^2-N_2CH(dmp)} (**3**, irrelevant H atoms omitted for clarity). Selected distances (Å) and angles (°): Ni–N(1) = 1.845(2), Ni–N(2) = 1.876(2), N(1)–N(2) = 1.257(2), Ni–P(1) = 2.1794(7), Ni–P(2) = 2.1655(6), N(1)–C(3) = 1.331(3), C(3)–C(41) = 1.451(3) C(3)–H = 0.93(2); P(1)–Ni–P(2) = 93.66(3), N(1)–Ni–N(2) = 39.46(7), P(1)–Ni–N(1) = 120.15(6), P(2)–Ni–N(2) = 106.94(6), N(2)–N(1)–C(3) = 139.0(2), N(1)–C(3)–C(41) = 124.2(2), N(1)–C(3)–H = 114.1(13), Ni–N(1)–C(3) = 149.12(15).

nickel center (sum of angles at Ni = 360.2°). The N–N bond of the diazo ligand lies in the P–Ni–P plane at a distance of 1.751 Å from Ni, with Ni–N(1) being 1.845(2) Å and Ni–N(2) 1.876(2) Å. The interaction between the diazo ligand and the metal center is not very strong: the N(1)–N(2) distance is 1.257(2) Å, in the range of a N–N double bond,[13,14] indicating the lack of significant backbonding from nickel to the N=N fragment. This interpretation is corroborated by the fact that the $\nu_{N=N}$ is shifted by only 81 cm^{-1} from the corresponding frequency in the free diazo compound (see above).

Nitrogen extrusion from **3** was not straightforward. Complex **3** was stable to prolonged heating; even after a week at 80 °C only a small amount was converted to the desired carbene, (dtbpe)Ni=CH(dmp) (**1**). The use of $Sm(OTf)_3$ as a catalyst[3,15,16] did not induce the formation of **1** either. It is likely that the steric congestion in **3** prevents the coordination of the Lewis acid to the nitrogen atom.

Since the thermal and Lewis acid treatments of **3** were not successful, a photochemical approach was sought. After exposing an NMR tube to a UV-light source (mercury lamp, 254 nm), the quantitative conversion of **3** to **1** was observed in a few minutes.[17,18] Complex **1** was synthesized on a preparative scale by using either a high-energy mercury UV lamp or a commercial "sun lamp"; no special quartz glassware was required (no difference was observed in a control experiment when employing both quartz and regular glassware vessels side by side).

The ^{1}H NMR spectrum of **1** features a specific downfield resonance for the α-hydrogen atom at 11.57 ppm, appearing as a triplet due to the coupling with the two phosphorus nuclei (J_{HP} = 15.2 Hz). In the ^{31}P NMR spectrum, the downfield singlet at 117.91 ppm is characteristic of a trigonal nickel carbene with the carbene substituents perpendicular to the coordination plane. The $^{13}C\{^1H\}$ NMR spectrum features a downfield-shifted carbene carbon at 205.9 ppm, as a triplet, with coupling to the two phosphorus nuclei (J_{CP} = 51.5 Hz); a doublet of triplets, with the coupling constant J_{CH} = 98.3 Hz (Figure 2),[19−24] was observed in the ^{1}H-coupled-^{13}C NMR spectrum, as a consequence of additional coupling with the hydrogen nucleus (shown in Figure 2).

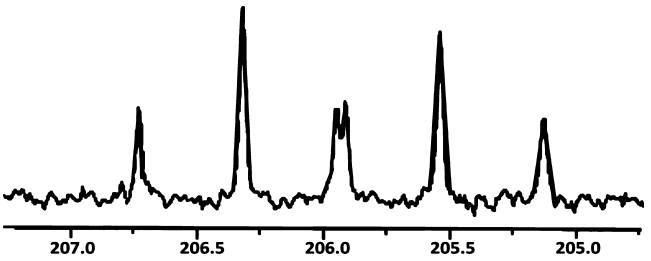

Figure 2. Downfield region of the ^{13}C NMR spectrum of **1**.

The solid-state molecular structure of **1** (Figure 3) supports the solution structural assignments. In addition, it was found that the new carbene has a shorter Ni–C distance (1.793(3) Å) compared to that of (dtbpe)Ni=CPh_2 (1.836(2) Å).[3] The bulky dmp substituent adopts a staggered conformation versus

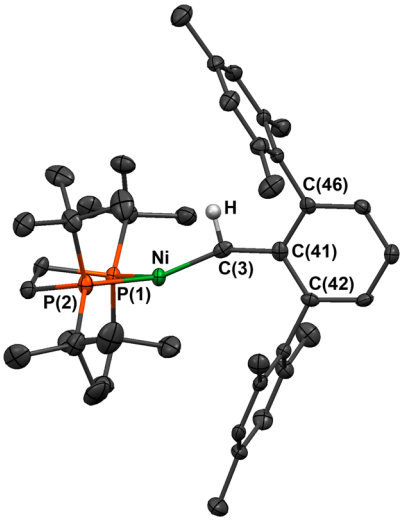

Figure 3. Thermal-ellipsoid (50% probability) representation of (dtbpe)Ni=CH(dmp) (**1**, irrelevant H atoms omitted for clarity). Selected distances (Å) and angles (°): Ni–C(3) = 1.793(3), Ni–P(1) = 2.1715(9), Ni–P(2) = 2.1763(10), C(3)–C(41) = 1.454(4), C(3)–H = 0.98(3); P(1)–Ni–P(2) = 91.60(4), P(1)–Ni–C(3) = 132.24(11), P(2)–Ni–C(3) = 129.84(11), Ni–C(3)–C(41) = 155.7(3), Ni–C(3)–H = 99.4(16), C(41)–C(3)–H = 105(2).

dx.doi.org/10.1021/ja501900j | J. Am. Chem. Soc. 2014, 136, 6479−6488

the dtbpe ligand, with the central phenyl ring almost perpendicular to the P(1)−Ni−P(2) plane (the dihedral angle between the P(1)−Ni−P(2) plane and the C(46)−C(41)−C(42) plane is 79.71°). The nickel center has a trigonal-planar geometry, with the sum of the angles around nickel being 353.68°, slightly lower than the expected 360°. The Ni−C bond is bisecting the P(1)−Ni−P(2) angle, but is shifted out of its plane by 26.97°. The α-hydrogen atom was located in the electronic density map, attached to the carbene carbon and at a distance of 0.98(3) Å from it, in agreement with the high J_{CH} coupling constant determined by ^{13}C NMR spectroscopy. The sum of the angles around the carbene carbon is 360°. Notably, the value observed for the Ni−C(3)−C(41) angle of 155.7° is high and falls between 120°, expected for an sp^2 hybridized carbon, and 180°, for an sp carbon. It is likely that this value is a consequence of the steric requirements imposed by the dmp substituent and the *t*-butyl groups: an NBO analysis of **1** indicates a bond order of 2 for Ni=C.

DFT calculations offered insight into the electronic structure of **1**. The HOMO of the carbene model complex (dmpe)N=C(H)Ph (dmpe = 1,2-bis(dimethylphosphino)ethane) is a bonding orbital of π symmetry between the $d_{x^2-y^2}$ orbital of nickel and the p_x orbital of carbon (Figure 4). The other frontier molecular orbitals also agree with the above bonding description: HOMO−4 is constituted by the σ Ni−C bond, while LUMO and LUMO+1 are the antibonding orbitals corresponding to the σ and π Ni−C bond, respectively (Figure 4).

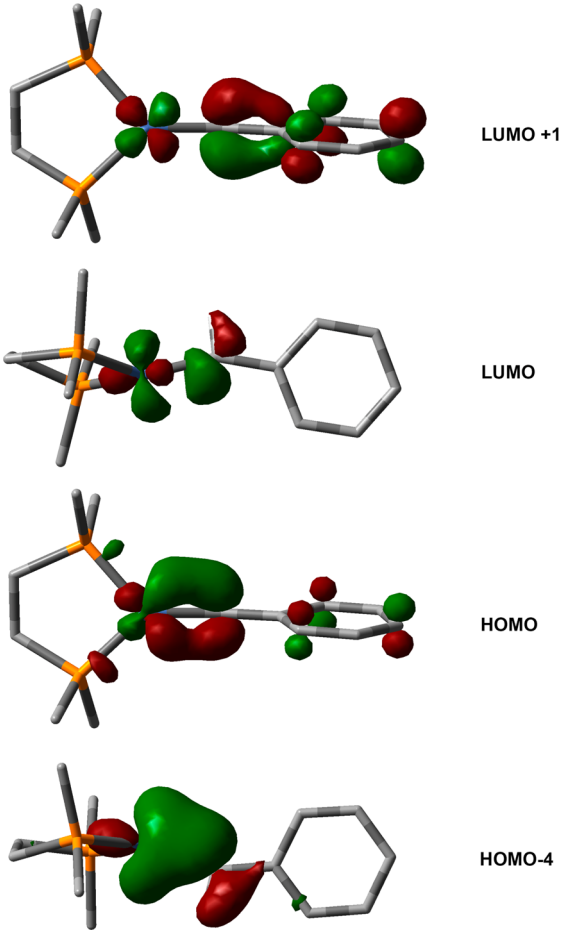

Figure 4. Frontier molecular orbitals for (dmpe)N=C(H)Ph, a computational model of **1**.

In order to determine whether a cationic nickel carbene is accessible, the oxidation of **1** was attempted. The reaction of a cold (−35 °C) diethyl ether solution of **1** with $[Cp_2Fe^+][B(Ar^F)_4^-]$ (Scheme 2) led to a new nickel cationic complex

Scheme 2. Oxidation of (dtbpe)Ni=CH(dmp) (1)[a]

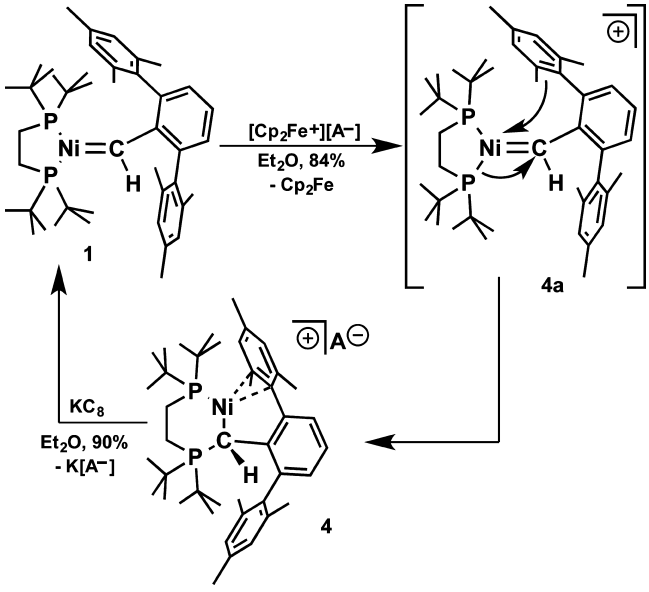

[a] A = $B(Ar^F)_4$.

formulated as [{κ^2-P,C-di-*tert*-butylphosphino-di-*tert*-butyl-PCH(dmp)ethane}Ni][$B(Ar^F)_4^-$] (**4**), in which one of the phosphine donors migrated to the carbene fragment generating an ylide during an intramolecular rearrangement. The light-yellow complex **4** has a magnetic moment of 2.1 μ_B in solution (measured by the Evans method)[25,26] that corresponds to one unpaired electron.

The single-crystal X-ray structure of **4** (Figure 5) revealed that the oxidation took place with an internal rearrangement. The Ni−C distance of 2.077(4) Å is longer than in **1** and in the range of Ni(I)−C alkyl single bonds.[27,28] One of the phosphorus atoms of the dtbpe ligand is still attached to nickel and one of the mesityl substituents from the dmp ligand is coordinated in an η^2 fashion. The C(321)−C(322) distance (1.432(5) Å) of the phenyl ring coordinated to nickel is slightly longer than a usual aromatic C−C distance (1.38 Å), but the aromaticity is not disrupted. This is the longest C−C distance; the other C−C distances of the phenyl ring vary between 1.371(5) and 1.424(5) Å. It is proposed that one of the phosphine branches of the dtbpe ligand in **4a** (Scheme 2) migrated from nickel to the carbene carbon, generating a phosphonium ion. The coordinative properties of ylides have been studied but it is interesting to note that ylide complexes are mostly synthesized from phosphonium ions by deprotonation.[29−32]

The rearrangement induced by the redox process is reversible. By treating **4** with a one-electron reducing agent (KC_8), the carbene **1** was obtained (Scheme 2). The reversible nature of the **1**-to-**4** conversion is supported by cyclic voltammetry data (Figure 6). A 10^{-2} M solution of **1** in 1 M [$^nBu_4N$][PF_6]/THF shows two quasi-reversible waves, at −0.61 and −2.76 V, and an irreversible wave, at −0.15 V (vs Fc/Fc^+).

dx.doi.org/10.1021/ja501900j | J. Am. Chem. Soc. 2014, 136, 6479−6488

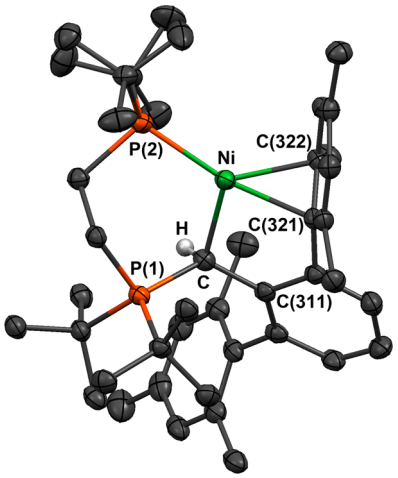

Figure 5. Thermal-ellipsoid (50% probability) representation of [{κ^2-P,C-di-*tert*-butylphosphino-di-*tert*-butyl-PCH(dmp)ethane}Ni][B-$(Ar^F)_4^-$] (**4**, irrelevant H atoms omitted for clarity). Selected distances (Å) and angles (°): Ni–C = 2.077(4), Ni–P(2) = 2.2275(12), Ni–C(321) = 2.136(4), Ni–C(322) = 2.092(4), C–P(1) = 1.811(4), C–C(311) = 1.538(5), C(321)–C(322) = 1.432(5); P(2)–Ni–C = 106.35(12), Ni–C–P(1) = 109.0(2), Ni–C–C(311) = 107.2(3), P(1)–C–C(311) = 125.5(3), C(321)–Ni–C(322) = 39.57(14).

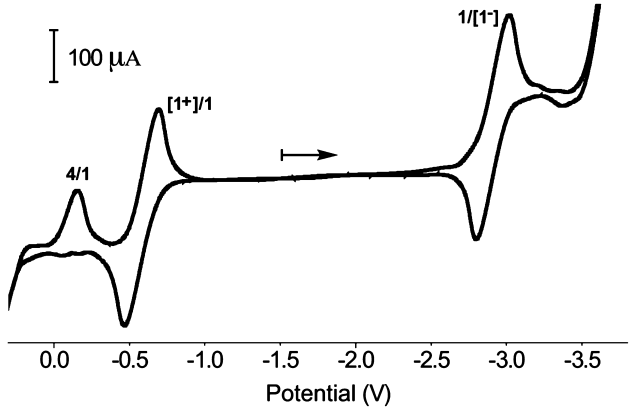

Figure 6. Cyclic voltammogram for (dtbpe)Ni=CH(dmp) (**1**) at 100 mV/s, 10 mM in 1 M [^{n}Bu$_4$N][PF$_6$] in THF, Cp_2Fe/Cp_2Fe^+ corrected.

The quasi-reversible waves were assigned to the [(dtbpe)Ni=CH(dmp)$^+$]/(dtbpe)Ni=CH(dmp) ($E_{1/2}$ = −0.61 V) and (dtbpe)Ni=CH(dmp)/[(dtbpe)Ni=CH(dmp)$^-$] ($E_{1/2}$ = −2.76 V) processes. These values are close to the corresponding values observed for (dtbpe)Ni=N(dmp) (−0.76 and −2.81 V, respectively) under similar conditions.[39] The irreversible wave (at −0.15 V) is consistent with the formation of a product resulting from the oxidation of (dtbpe)Ni=CH(dmp) and present in solution along [(dtbpe)-Ni=CH(dmp)$^+$]. This wave, present at low-speed scanning rates, loses intensity at scanning rates higher than 100 mV/s. We tentatively assign this to the oxidation of **4**, an intermediate not observed at fast scanning rates.

Removal of the carbene hydrogen of **1** could, in principle, generate a nickel carbyne species. The bulky, stable radical 1,3,5-tri-*tert*-butylphenoxyl[33−35] (^{S}MesO$^\bullet$) has been used successfully in removing the hydrogen atom from both the amide (dtbpe)Ni–NH(dmp) and the phosphide (dtbpe)Ni–PH(dmp).[36] The carbene **1**, however, does not react with ^{S}MesO$^\bullet$ even after extended periods of time at increased temperatures. This lack of reactivity is likely not related to steric factors, since the same reagent abstracts hydrogen from (dtbpe)Ni–NH(dmp) and (dtbpe)Ni–PH(dmp),[36] but to a higher dissociation energy of the C–H compared to the N–H and P–H bonds.[37] Complex **1** also exhibits an unusual chemical inertia toward strong bases; it did not react with ^{n}BuLi, $(Me_3Si)_2NNa$, $^i Pr_2NLi$, or CH_3Li even at 80 °C.

It is possible that the internal redistribution of electrons to give a Ni(I) complex is favored by the dissociation of one of the phosphines. It was reasoned that replacing the ethylene backbone with a 1,8-naphthylene spacer might prevent phosphine dissociation. Although 6-member rings are considered to be less stable than 5-member rings, the formation of a 6-member nickel species may prevent the rearrangement process, since the 1,8-naphthylene ligand would lead to the formation of a 7-member ring, likely an unfavorable process.

The second factor that could prevent the rearrangement identified during the oxidation of **1** is kinetic. An equilibrium between the complex with the ligand coordinated in a chelating fashion and the complex with the ligand coordinated in a monodentate fashion exists in solution. The chelated species is favored, but the equilibrium can be shifted away from it if additional donors are present. The coordination of dtbpe as a monodentate or bridging ligand was observed in several instances.[11] During the rearrangement of **4a**, the migration of the phosphine ligand from nickel to carbon might involve such a process. Replacing the ethylene backbone with 1,8-naphthylene would make this ligand rigid. Even in the extreme case of monodentate coordination, the other phosphine arm is forced to stay in close proximity. The rotation around the P–$C_{naphthalene}$ bond is also hindered, making the switch between monodentate and bidentate coordination unlikely.

Consequently, a Ni(0) precursor, (dippn)Ni(cod), was synthesized and characterized.[38] The complex (dippn)Ni(cod) reacts cleanly (Scheme 3) and in high yield with $(dmp)CHN_2$.

Scheme 3. Formation of (dippn)Ni=CH(dmp) (2)

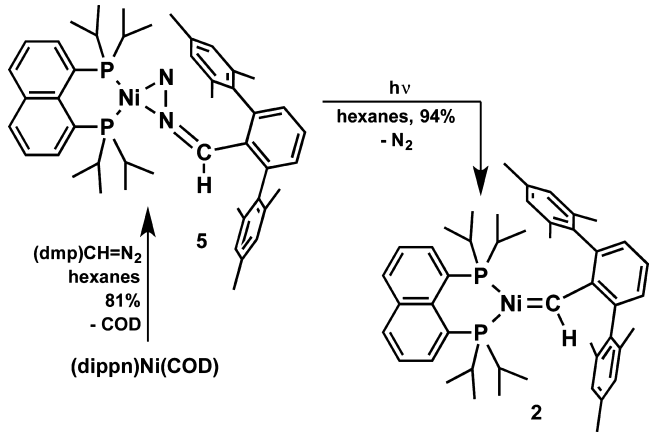

The reaction was performed in the dark to avoid the decomposition of the Ni(0) product, (dippn)Ni{*N,N*-η^2-$N_2CH(dmp)$} (**5**). The complex **5** can be readily isolated due to its insolubility in pentanes. Its infrared spectrum features a $\nu_{C=N}$ stretch at 2055 cm^{-1} and a $\nu_{N=N}$ stretch at 1512 cm^{-1} (compared to 2052 cm^{-1} and, respectively, 1437 cm^{-1} in free $(dmp)CHN_2$), a good indication for the η^2 coordination of the N=N double bond. The key structural parameters describing

dx.doi.org/10.1021/ja501900j | J. Am. Chem. Soc. 2014, 136, 6479−6488

the geometry of the nickel center obtained from the solid-state structure of **5** (Figure 7) are similar to those of **3**. The nickel

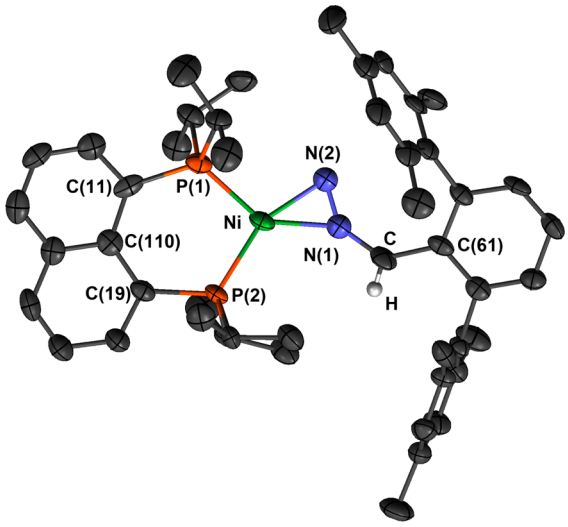

Figure 7. Thermal-ellipsoid (50% probability) representation of (dippn)Ni{η^2-N_2CH(dmp)} (**5**, irrelevant H atoms omitted for clarity). Selected distances (Å) and angles (°): Ni–N(2) = 1.883(5), Ni–N(1) = 1.909(5), Ni–P(1) = 2.124(2), Ni–P(2) = 2.1361(15), N(1)–N(2) = 1.212(6), N(1)–C = 1.359(7); P(1)–Ni–P(2) = 99.98(7), N(1)–Ni–N(2) = 37.3(2), P(1)–Ni–N(2) = 104.68(15), P(2)–Ni–N(1) = 118.1(2), N(2)–N(1)–C = 142.0(6), N(1)–C–C(61) = 131.7(6).

center is planar and the two phosphorus atoms, Ni, and the two nitrogen atoms are coplanar. The imine hydrogen atom was located in the electron density map at 0.82 Å from carbon.

By exposing a diethyl ether solution of **5** to ultraviolet light (either a "sun-lamp" or a mercury lamp) for several days, dinitrogen was lost and the new carbene (dippn)Ni=CH(dmp) (**2**) could be isolated in a quantitative yield as bright emerald-green crystals (Scheme 3). The reaction is very clean; no byproducts were observed and no decomposition occurred when the reaction mixture was kept at room temperature.

The ^{1}H NMR spectrum of **2** indicated that the carbene proton appeared downfield, at 12.21 ppm, as a triplet due to coupling to the two phosphorus nuclei. The spectroscopic resemblance between **2** and **1** was also observed in the solid-state structure. The single-crystal data (Figure 8) revealed that the Ni–C distance (1.797(3) Å) has, within errors, the same value for both carbenes, while the Ni–C–C angle (152.3(3)°) is slightly smaller for **2** than for **1**. The metal center is pseudotrigonal planar, with the sum of angles of 356.43° around nickel, slightly off the planar requirements, possibly a consequence of the small displacement of the Ni–C bond from the phosphine ligand plane (by 23.1°). The carbene hydrogen atom was located in the electron density map at 1.02(3) Å from the carbon atom. Interestingly, the dmp substituent is in a twisted conformation with respect to the dippn ligand (Figure 8). For the analogous carbene **1**, the two mesityls are in a staggered conformation with the dtbpe ligand (*vide supra*), but in **2** the dihedral angle between the P(1)–Ni–P(2) plane and the C(62)–C(11)–C(66) plane is 46.2° indicating a conformation between staggered and eclipsed. Also noticeable from the space-filling model (Figure 9) is the problematic fitting of the *iso*-propyl substituents on the phosphine ligand.

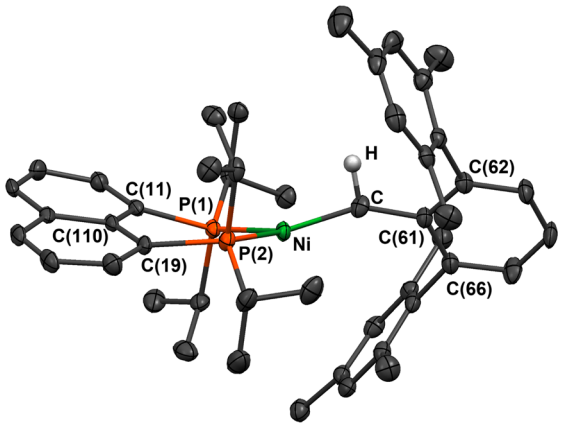

Figure 8. Thermal-ellipsoid (50% probability) representation of (dippn)Ni=CH(dmp) (**2**, irrelevant H atoms omitted for clarity). Selected distances (Å) and angles (°): Ni–C = 1.797(3), Ni–P(1) = 2.1322(10), Ni–P(2) = 2.1344(10), C–C(61) = 1.457(4), C–H = 1.02(3); P(1)–Ni–P(2) = 96.52(4), P(1)–Ni–C = 126.12(10), P(2)–Ni–C = 133.79(11), Ni–C–C(61) = 152.3(3), Ni–C–H = 97.5(16).

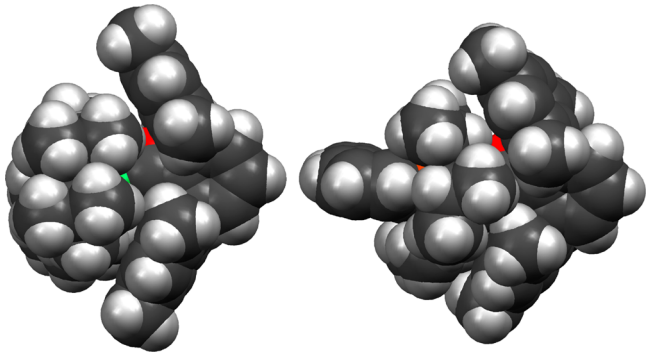

Figure 9. Space-filling models for **1** and **2**.

This steric repulsion determines the magnetic nonequivalence of the methyl groups of the *iso*-propyl substituents even in solution, as observed in the ^{1}H NMR spectra of **2**.

The new carbene **2** is a robust complex and not very reactive; short exposure of the crystalline material or its solution to air or water does not affect its integrity. The chemical stability of **2** is likely due to the extremely bulky ligands protecting the core of the complex. Additionally, common strong bases (MeLi, *n*-butyllithium, $(Me_3Si)_2NNa$, or KH) do not react with it, and abstraction of the hydrogen atom as a radical using ^{S}MesO$^\bullet$ was not possible.

The cyclic voltammogram of **2** (Figure 10), measured for a 0.01 M THF solution, features two quasi-reversible events at −0.75 V and −3.85 V (vs Fc/Fc$^+$) that were assigned to the [(dippn)Ni=CH(dmp)$^+$]/ (dippn)Ni=CH(dmp) and (dippn)Ni=CH(dmp)/[(dippn)Ni=CH(dmp)$^-$] redox couples. No irreversible features, as found for **1**, were detected at low scan rates for **2**. Accordingly, the oxidation of **2** using $[Cp_2Fe^+][B(Ar^F)_4^-]$ led to the isolation of a new paramagnetic complex, formulated as the cationic nickel(III) carbene [(dippn)Ni{CH(dmp)}$^+$][$B(Ar^F)_4^-$] (**6**), as a light-pink powder (Scheme 4). Unfortunately, all the attempts to grow single crystals of **6** suitable for X-ray diffraction were not successful.

Complex **6** is a one-electron paramagnet as indicated by its room-temperature μ_{eff} of 2.0 μ_B, measured in a CD_2Cl_2 solution

dx.doi.org/10.1021/ja501900j | J. Am. Chem. Soc. 2014, 136, 6479–6488

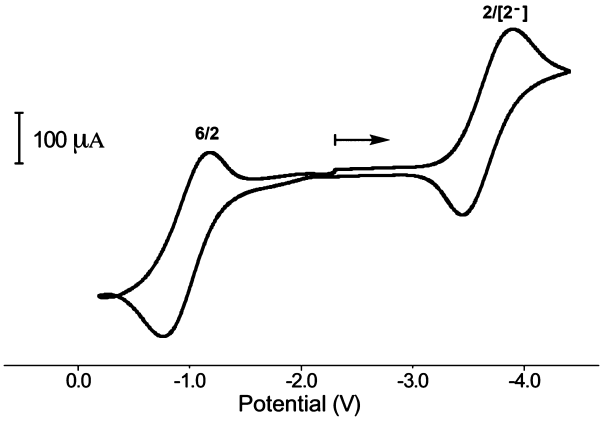

Figure 10. Cyclic voltammogram for (dippn)Ni=CH(dmp) (**2**) at 100 mV/s, 10 mM in 1 M $[^nBu_4N][PF_6]$ in THF, Cp_2Fe/Cp_2Fe^+ corrected.

Scheme 4. Formation of $[(dippn)Ni\{CH(dmp)\}^+][B(Ar^F)_4^-]$ (6)[a]

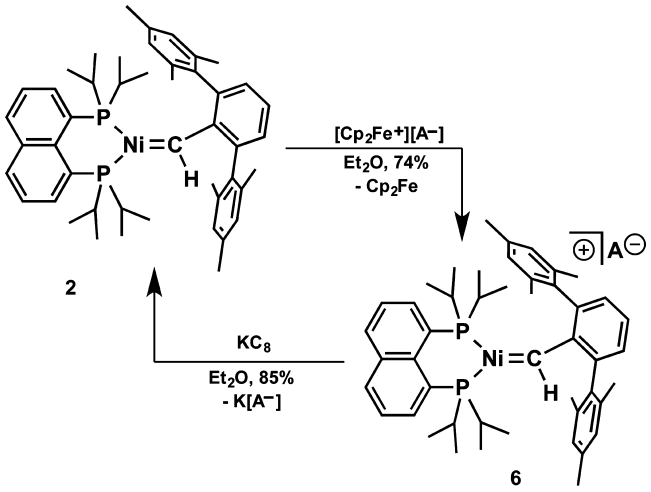

[a] A = $B(Ar^F)_4$.

by the Evans method, and variable-temperature solid-state measurements (using a superconducting quantum interference device). Although two electron configurations are possible for a d^7 trigonal-planar ion, high spin with three unpaired electrons and low spin with one unpaired electron, both the solution and the solid-state magnetization measurements indicate the presence of one unpaired electron (Figure 11). Similar results were obtained for the cationic nickel imide $[(dtbpe)Ni{=}N(dmp)^+][B(Ar^F)_4^-]$, which has a low-spin configuration.[39]

Complex **6** was characterized further by EPR spectroscopy (Figure 12). The EPR X-band spectrum of **6** (1 mM in CH_2Cl_2) at 5 K is also consistent with the presence of an unpaired electron on the nickel center.[40] The spectrum exhibits a rhombic band, with unresolved hyperfine structure likely due to ^{31}P delocalization and is centered around g = 2.2. Overall, the EPR spectrum of **6** shows similar features to that of $[(dtbpe)Ni{=}N(dmp)^+][B(Ar^F)_4^-]$.[39]

DFT calculations support the assignment of **6** as $[(dippn)Ni{=}CH(dmp)^+][B(Ar^F)_4^-]$ as follows. When the total bonding energy of the putative carbene $[(dtbpe)Ni{=}CH(dmp)^+]$ ([**4a**]) was compared to that of **4**, it was found that **4** is more stable than [**4a**] by −8.4 kcal/mol. The same

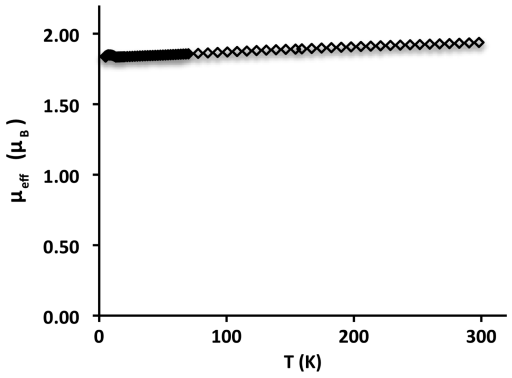

Figure 11. Solid-state magnetization data for $[(dippn)Ni{=}CH(dmp)^+][B(Ar^F)_4^-]$ (**6**) as a function of temperature (5−300 K, 5000 G).

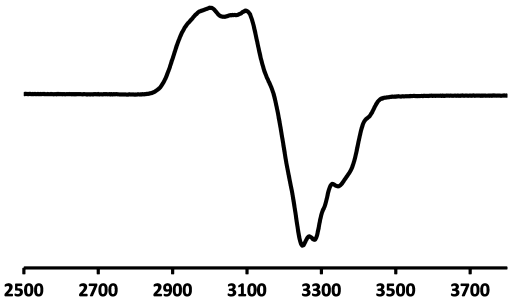

Figure 12. EPR spectrum (1 mM in CH_2Cl_2, 5 K) of $[(dippn)Ni{=}CH(dmp)^+][B(Ar^F)_4^-]$ (**6**).

comparison indicates that $[(dippn)Ni{=}CH(dmp)^+]$ (**6**) is more stable than the presumed rearranged product [**6a**] by −22.8 kcal/mol. These values are in agreement with the fact that **6** features a more rigid ligand than **4** and is less likely to rearrange to a nickel(I) alkyl phosphonium product, as was observed for **4** (Figure 13).

CONCLUSIONS

In conclusion, two new nickel carbenes, (dtbpe)Ni=CH(dmp) (**1**) and (dippn)Ni=CH(dmp) (**2**), were isolated and characterized. To stabilize these species, dmp (2,6-dimesityl-

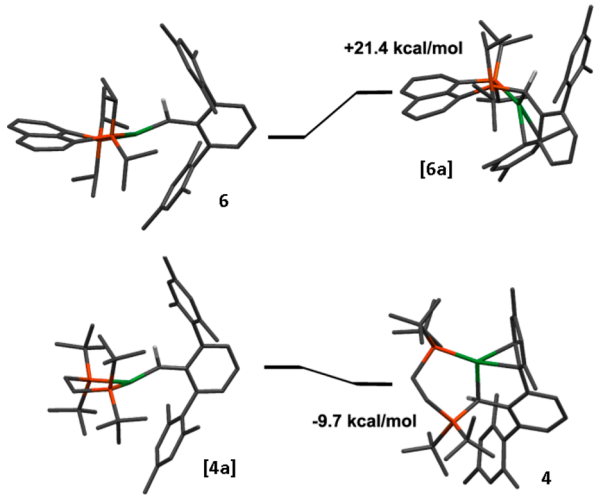

Figure 13. Calculated free energies (kcal/mol) for the rearrangement of **6** to [**6a**] (top) and [**4a**] to **4** (bottom).

dx.doi.org/10.1021/ja501900j | J. Am. Chem. Soc. 2014, 136, 6479−6488

phenyl) was employed to offer the necessary steric protection to the metal core. The other carbene substituent is hydrogen. Structurally, **1** and **2** were characterized by short Ni−C distances and Ni−C−C angles at the carbene carbon that are intermediate between 120° and 180° (155.7° and 152.3(3)°, respectively). Attempts to oxidize **1** and/or to abstract its carbene hydrogen did not lead to the formation of a carbene or carbyne moiety. Instead, phosphorus migration from nickel to the carbene carbon occurred, leading to the formation of a Ni(I) ylide complex, **4**. In contrast, the oxidation of **2** led to a product formulated as $[(\text{dippn})\text{Ni}{=}\text{CH}(\text{dmp})^+][\text{B}(\text{Ar}^\text{F})_4^-]$ (**6**). Complex **6** was characterized by solution and solid-state magnetization studies and EPR spectroscopy, which indicate that its electronic configuration is similar to that of the cationic nickel(III) imide $[(\text{dtbpe})\text{Ni}{=}\text{N}(\text{dmp})^+][\text{B}(\text{Ar}^\text{F})_4^-]$. DFT calculations supported that assignment. The formation of the cationic nickel(III) carbene species took advantage of the steric characteristics of the dippn supporting ligand, featuring a rigid, 1,8-naphthylene backbone, which does not allow its rearrangement, as observed for the dtbpe ligand.

EXPERIMENTAL SECTION

Unless noted otherwise, all operations were performed under a purified nitrogen atmosphere in a standard MBraun Lab Master 130 drybox or under an argon atmosphere using high-vacuum and Schlenk techniques.[41] Hexanes, petroleum ether, and toluene were dried by passage through activated alumina and Q-5 columns under nitrogen.[42] CH_2Cl_2 was dried by distillation from CaH_2 or passed twice through activated alumina columns. THF was distilled from a dark-purple THF solution of sodium benzophenone ketyl. Anhydrous diethyl ether was stirred for 24 h over metallic sodium and filtered under nitrogen through an activated alumina plug. Benzene was refluxed under nitrogen over CaH_2 and distilled. CD_2Cl_2 and C_6D_6 were purchased from Cambridge Isotope Laboratory, degassed, dried over CaH_2, transferred under vacuum, and stored over 4 Å molecular sieves. Four Å molecular sieves, alumina, silica, and Celite were dried under dynamic vacuum overnight at 180 °C. Q-5 was activated by heating at 200 °C under a 5% H_2 in N_2 atmosphere. Unless noted, chemicals were purchased from commercial sources and used without further purification. KC_8,[43] $(\text{dmp})\text{C(H)N}_2$,[12] $[\text{Cp}_2\text{Fe}][\text{B}(3,5\text{-}(\text{CF}_3)_2\text{C}_6\text{H}_3)_4]$,[44] $[(\text{dtbpe})\text{Ni}]_2(\text{C}_6\text{H}_6)$,[45] (dippn)Ni(COD),[38] and $^\text{S}$MesO[33−35] were prepared according to the literature. All NMR spectra were recorded using a Bruker DRX-400 or DRX-500 spectrometer. ^{1}H NMR spectra were referenced to solvent residual peaks at δ 7.16 for C_6D_6, and δ 5.32 for CD_2Cl_2. ^{31}P NMR spectra were measured using a 250 ppm window and offset referenced to an external standard, 85% phosphoric acid (δ 0.00 ppm). ^{13}C NMR spectra were acquired using the pulse-Fourier technique. Proton-decoupled spectra were collected with Walts decoupling. ^{13}C NMR spectra were referenced to solvent residual peaks, δ 128.0 for C_6D_6 and δ 53.8 for CD_2Cl_2. Infrared spectra were measured as Fluorolube-S20 or Nujol mulls between CaF_2 or KBr plates using a Nicolet 20-SXB spectometer with TGS detector. Solution magnetic susceptibilities were calculated using the Evans method[25,26] using trimethylsilyl ether as an internal standard. Elemental analyses were performed by Columbia Analytics (Tucson, AZ) or by Midwest Microlab (Indianapolis, IN). Cyclic voltametry experiments were carried out on an Eco-Chemie Autolab potentiostat. EPR spectra were collected on a BrukerEMX EPR spectrometer. Magnetic susceptibility measurements were carried out on batches obtained independently until at least two different experiments gave superimposable results. Magnetic susceptibility measurements were recorded using a SQUID magnetometer at 5000 G.

Synthesis of (dtbpe)Ni{η^2-N_2CH(dmp)} (3). To a suspension of 83.4 mg (0.1 mmol) of $[(\text{dtbpe})\text{Ni}]_2(\mu\text{-}C_6H_6)$ in 5 mL of *n*-pentane was added a solution of 70.9 mg (0.2 mmol) of $(\text{dmp})\text{C(H)N}_2$ in 5 mL of *n*-pentane. The mixture was stirred for 2 h at room temperature. The resulting yellow precipitate was suspended in 5 mL *n*-pentane, filtered, washed 3 times with 1 mL of *n*-pentane, and dried under reduced pressure to yield 131.7 mg (0.18 mmol, 90%) of pure **3** as a yellow crystalline powder. Single crystals suitable for X-ray diffraction analysis were obtained by the slow crystallization of a diluted solution of **3** in *n*-pentane at −35 °C. For **3**: ^{1}H NMR (20 °C, 500.13 MHz, C_6D_6): δ 7.16 (m, 3H, C_6H_3), 6.93 (s, 4H, C_6H_2), 5.37 (d, J_{HP} = 6.0 Hz, 1H, C*H*═N), 2.40 (s, 12H, CH_3), 2.32 (s, 6H, CH_3), 1.08 (m, 4H, CH_2), 1.03 (d, J_{HP} = 12 Hz, 18H, $C(CH_3)_3$), 0.88 (d, J_{HP} = 12 Hz, 18H, $C(CH_3)_3$). ^{31}P{^{1}H} NMR (20 °C, 202.47 MHz, C_6D_6): δ 91.91 (d, J_{PP} = 63.2 Hz), 88.98 (d, J_{PP} = 63.2 Hz). ^{13}C{^{1}H} NMR (20 °C, 125.77 MHz, C_6D_6): δ 140.69 (s, C_{Ar}), 137.28 (s, C_{Ar}), 136.70 (s, C_{Ar}), 136.45 (s, C_{Ar}), 134.51 (s, C_{Ar}), 129.21 (s, C_{Ar}), 128.59 (s, C_{Ar}), 123.09 (s, C_{Ar}), 85.50 (t, J_{CP} = 9.7 Hz, CH═N), 34.21 (dd, J_{CP} = 12.0 Hz, J_{CP} = 12.0 Hz, CH_2), 33.81 (dd, J_{CP} = 12.0 Hz, J_{CP} = 12.0 Hz, CH_2), 30.16 (t, J_{CP} = 7.8 Hz, $C(CH_3)_3$), 22.74 (t, J_{CP} = 15.9 Hz, $C(CH_3)_3$), 21.87 (t, J_{CP} = 15.9 Hz, $C(CH_3)_3$), 21.49 (s, CH_3), 21.35 (s, CH_3). IR (CaF_2, Fluorolube): 2997 (m), 2974 (m), 2943 (m), 2912 (m), 2863 (m), 2058 (w, $\nu_{C=N}$), 1519 (s, $\nu_{N=N}$), 1477 (m), 1420 (m) cm^{-1}. Elemental analysis for $C_{43}H_{66}N_2NiP_2$: C% 70.59, H% 9.09 N% 3.83; found C% 71.13, H% 8.82, N% 3.84.

Synthesis of (dtbpe)Ni═CH(dmp) (1). A 50 mL airtight Pyrex glass flask was charged with 146.3 mg (0.2 mmol) of (dtbpe)Ni{η^2-N_2CH(dmp)} (**3**) and 10 mL of hexanes, cooled to −78 °C, and evacuated to 1 mmHg. The flask was exposed for 12 h to a 275 W General Electric sun lamp with continuous air cooling to keep the mixture at room temperature. The resulting emerald-green solution was concentrated to dryness under reduced pressure to yield analytically pure **1** (140.73 mg, 0.2 mmol, 100%) as a dark-green crystalline powder. For **1**: ^{1}H NMR (20 °C, 400.13 MHz, C_6D_6): δ 11.57 (t, J_{HP} = 15.2 Hz, 1H, Ni═C*H*(dmp)), 7.89 (tt, J_{HH} = 7.4 Hz, J_{HP} = 3.7 Hz, 1H, *p*-C_6H_3), 6.95 (s, 4H, C_6H_2), 6.89 (d, J_{HH} = 7.4 Hz, 2H, *m*-C_6H_3), 2.31 (s, 6H, CH_3), 2.26 (s, 12H, CH_3), 1.90 (d, J_{HP} = 11.7 Hz, 18H, $C(CH_3)_3$), 1.21 (m, 2H, CH_2), 0.98 (d, J_{HP} = 11.7 Hz, 18H, $C(CH_3)_3$), 0.87 (m, 2H, CH_2). ^{31}P{^{1}H} NMR (20 °C, 161.98 MHz, C_6D_6): δ 117.91 (s). ^{13}C{^{1}H} NMR (20 °C, 100.62 MHz, C_6D_6): δ 205.93 (t, J_{CP} = 51.5 Hz, Ni═CH(dmp)) 158.30 (d, J_{CP} = 7.5 Hz, C_{Ar}), 144.22 (s, C_{Ar}), 140.40 (m, C_{Ar}), 134.87 (s, C_{Ar}), 134.54 (s, C_{Ar}), 131.12 (d, J_{CP} = 7.2 Hz, C_{Ar}), 129.29 (s, C_{Ar}), 124.36 (s, C_{Ar}), 34.09 (m, $C(CH_3)_3$), 33.41 (m, $C(CH_3)_3$), 31.06 (s, $C(CH_3)_3$), 30.48 (s, $C(CH_3)_3$), 22.38 (m, CH_2), 21.5 (s, CH_3), 21.37 (s, CH_3). ^{13}C NMR (20 °C, 125.77 MHz, C_6D_6): δ 205.9 (dt, J_{CP} = 51.5 Hz, J_{CH} = 98.3 Hz, Ni═CH(dmp)). Elemental analysis for $C_{43}H_{66}NiP_2$: C% 73.40; H% 9.45; found: C% 73.24, H% 9.26.

Synthesis of [{κ^2-P,C-di-*tert*-butylphosphino-di-*tert*-butyl-PCH(dmp)ethane}Ni][BAr^F_4] (4). A cold (−35 °C) solution of $[\text{Cp}_2\text{Fe}^+][\text{B}(\text{Ar}^\text{F})_4^-]$ (52.46 mg, 0.05 mmol in 5 mL of Et_2O) was added dropwise to a solution of **1** (35.2 mg, 0.05 mmol in 5 mL of Et_2O) at −35 °C. The mixture was stirred at room temperature for 30 min. After removing the volatiles under reduced pressure, the residue was triturated 5 times with 5 mL of *n*-pentane. Dissolving the residue in 5 mL of Et_2O and layering the solution with *n*-pentane at −35 °C induced crystallization. Subsequent filtration led to pure **4** (65.80 mg, 0.042 mmol, 84%). For **4**: ^{1}H NMR (20 °C, 400.13 MHz, CD_2Cl_2): δ 20.91 (b, $\Delta_{1/2}$ = 250 Hz, 18H, $C(CH_3)_3$), 8.72 (br, $\Delta_{1/2}$ = 230 Hz, 18H, $C(CH_3)_3$), 7.74 (s, 8H, $C_6H_2(CF_3)_2$), 7.57 (s, 4H, $C_6H_2(CF_3)_2$), 6.34 (br, $\Delta_{1/2}$ = 120 Hz, 4H, C_2H_4), 6.25 (br, $\Delta_{1/2}$ =70 Hz, 3H, $C_6H_2(CH_3)_3$), 5.33 (b, $\Delta_{1/2}$ = 70 Hz, 6H, $C_6H_2(CH_3)_3$), 1.72 (br, $\Delta_{1/2}$ = 50 Hz, 6H, $C_6H_2(CH_3)_3$), 1.15 (br, $\Delta_{1/2}$ = 50 Hz, 3H, $C_6H_2(CH_3)_3$), 0.95 (br, $\Delta_{1/2}$ = 80 Hz, 3H, $C_6H_2(CH_3)_3$), 0.09 (br, $\Delta_{1/2}$ = 50 Hz, 1H, C*H*(dmp)), 2.4 (br, $\Delta_{1/2}$ = 180 Hz, 4H, C_6H_3). IR (CaF_2, Fluorolube): 3177 (m), 2959 (m), 1611 (w), 1479 (m), 1354 (s) cm^{-1}. Magnetic moment (Evans, CD_2Cl_2, 20 °C): μ_{eff} = 2.1 μB. Elemental analysis for $C_{75}H_{78}NiP_2BF_{24}$: C% 57.49; H% 5.02; found: C % 56.46, H% 5.36.

Reduction of [{κ^2-P,C-di-*tert*-butylphosphino-di-*tert*-butyl-PCH(dmp)ethane}Ni][BAr^F_4] (4). A cold (−35 °C) suspension of KC_8 (5 mg, 0.037 mmol) in 2 mL of Et_2O was added dropwise to a solution of [{κ^2-P,C-di-*tert*-butylphosphino-di-*tert*-butyl-PCH(dmp)-ethane}Ni][BAr^F_4] (**4**, 58 mg, 0.037 mmol in 5 mL Et_2O) at −35 °C.

dx.doi.org/10.1021/ja501900j | J. Am. Chem. Soc. 2014, 136, 6479−6488

The mixture was stirred at room temperature for 30 min. The solution was concentrated to dryness and the black residue was suspended in 10 mL of hexanes. The black suspension was filtered through a plug of Celite. Cooling the solution at −35 °C induced the crystallization of **1**. The emerald-green crystals of (dtbpe)Ni=CH(dmp) (**1**, 25 mg, 0.035 mmol 95%) were isolated by decanting the mother liquor and dried under reduced pressure.

Synthesis of (dippn)Ni{η^2-N_2CH(dmp)} (5). To a suspension of 105 mg (0.2 mmol) of (dippn)Ni(COD) in 5 mL of *n*-pentane was added a solution of 71 mg (0.2 mmol) of (dmp)C(H)N_2 in 5 mL of *n*-pentane. The mixture was stirred for 2 h at ambient temperature. The resulting dark-yellow precipitate was filtered, washed 3 times with 1 mL of *n*-pentane, and dried under reduced pressure to yield 125 mg (0.16 mmol, 81%) of pure **5** as a yellow, crystalline powder. For **5**: ^{1}H NMR (298 K, 500.13 MHz, C_6H_6): δ 7.45 (m, 2H, C_6H_8), 7.35 (t, J_{HH} = 8 Hz, 1H, C_6H_8), 7.11 (m, 3H, C_6H_3), 7.05 (t, J_{HH} = 8 Hz, 1H, C_6H_8), 7.02 (t, J_{HH} = 8 Hz, 2H, C_6H_8), 6.92 (s, 4H, $C_6H_2(CH_3)_3$), 5.49 (d, J_{HP} = 5 Hz, 1H, C*H*(dmp)), 2.39 (s, 12H, $C_6H_2(CH_3)_3$), 2.28 (s, 6H, $C_6H_2(CH_3)_3$), 2.05 (m, 2H, $CH(CH_3)_2$), 1.85 (m, 2H, $CH(CH_3)_2$), 1.20 (dd, J_{HP} = 15 Hz, J_{HH} = 7 Hz, 6H, $CH(CH_3)_2$), 0.83 (m, 12H, $CH(CH_3)_2$), 0.69 (dd, J_{HP} = 15 Hz, J_{HH} = 7 Hz, 6H, $CH(CH_3)_2$); ^{31}P{^{1}H} NMR (298 K, 202.5 MHz, C_6H_6): δ 46.47 (d. J_{PP} = 9 Hz), 43.78 (d, J_{PP} = 9 Hz); ^{13}C{^{1}H} NMR (298 K, 125.77 MHz, C_6H_6): δ 140.78 (s, C_{Ar}), 140.31 (s, C_{Ar}), 140.54 (s, C_{Ar}), 137.07 (s, C_{Ar}), 136.36 (s, C_{Ar}), 136.12 (m, C_{Ar}), 135,71 (m, C_{Ar}), 134.36 (s, C_{Ar}), 132.31 (s, C_{Ar}), 132.14 (s, C_{Ar}), 132.02 (s, C_{Ar}), 129.03 (s, C_{Ar}), 127.97 (s, C_{Ar}), 123.88 (d, 4.5 Hz, C_{Ar}), 122.93 (s, C_{Ar}), 87.68 (t, J_{CP} = 9.8 Hz, N_2C*H*(dmp)), 28.04 (d, J_{CP} = 14.5 Hz, $CH(CH_3)_2$), 27.55 (d, J_{CP} = 20.4 Hz, $CH(CH_3)_2$), 21.08 (s, $C_6H_2(CH_3)_2$), 21.03 (s, $C_6H_2(CH_3)_2$), 19.42 (d, J_{CP} = 9.8 Hz, $CH(CH_3)_2$), 19.24 (d, J_{CP} = 3.8 Hz, $CH(CH_3)_2$), 19.02 (d, J_{CP} = 3.9 Hz, $CH(CH_3)_2$), 18.23 (d, J_{CP} = 5.8 Hz, $CH(CH_3)_2$); IR (CaF_2, fluorolube): 2055 (w, $\nu_{C=N}$), 1512 (s, $\nu_{N=N}$) cm^{-1}. Elemental analysis for $C_{47}H_{60}N_2Ni$: C% 72.57; H% 7.82; N% 3.62 found: C% 72.33, H% 8.04, N% 3.50.

Synthesis of (dippn)Ni=CH(dmp) (2). A solution of **5** (155 mg, 0.2 mmol) in 50 mL of hexanes was exposed for 72 h to a UV light source (250 W, GE Sun-Lamp) with constant air cooling in an airtight 100 mL glass bomb. Several aliquots were analyzed by NMR spectroscopy to determine the reaction completion. The resulting emerald-green solution was transferred to a flask in the drybox, filtered through a plug of Celite, and the volatiles were removed under reduced pressure. The dark-green, crude product was analytically pure **2**. Isolated yield: 140 mg, 94%. For **2**: ^{1}H NMR (298 K, 500.13 MHz, C_6H_6): δ 12.21 (t, J_{HP} = 16 Hz, 1H, C*H*(dmp)), 7.66 (m, 1H, $C_6H_3Mes_2$), 7.47 (d, J_{HH} = 8 Hz, 2H, $C_6H_3Mes_2$), 7.63 (t, J_{HH} = 7 Hz, 2H, $C_{10}H_8$), 7.06 (t, J_{HH} = 7 Hz, 2H, $C_{10}H_8$), 6.98 (d, J_{HH} = 7 Hz, 2H, $C_{10}H_8$), 6.93 (s, 4H, $C_6H_2(CH_3)_3$), 2.35 (s, 12H, $C_6H_2(CH_3)_3$), 2.21 (s, 6H, $C_6H_2(CH_3)_3$), 1.96 (m, 2H, $CH(CH_3)_2$), 1.84 (m, 2H, $CH(CH_3)_2$), 0.77 (m, 24 H, $CH(CH_3)_2$); ^{31}P{^{1}H} NMR (298 K, 202.5 MHz, C_6H_6): δ 61.49 (s); ^{13}C{^{1}H} NMR (298 K, 125.77 MHz, C_6H_6): δ 215.82 (t, J_{CP} = 62 Hz, C*H*(dmp)), 143.25 (s, C_{Ar}), 140.09 (s, C_{Ar}), 138.71 (s, C_{Ar}), 135.36 (s, C_{Ar}), 145.17 (s, C_{Ar}), 134.87 (s, C_{Ar}), 131.50 (s, C_{Ar}), 131.22 (s, C_{Ar}), 130.68 (s, C_{Ar}), 130.64 (s, C_{Ar}), 130.61 (s, C_{Ar}), 125.21 (s, C_{Ar}), 124.53 (s, C_{Ar}), 124.48 (s, C_{Ar}), 124.44 (s, C_{Ar}), 123.90 (s, C_{Ar}), 26.00 (d, 8 Hz, $CH(CH_3)_2$), 25.17 (d, J_{CP} = 8 Hz, $CH(CH_3)_2$), 21.85 (s, $C_6H_2(CH_3)_2$), 21.0 (s, $C_6H_2(CH_3)_2$), 19.98 (s, $CH(CH_3)_2$), 19.46 (s, $CH(CH_3)_2$), 18.81 (s, $CH(CH_3)_2$), 17.99 (s, $CH(CH_3)_2$). Elemental analysis for $C_{47}H_{60}NiP_2$: C% 75.71; H% 8.11; found: C% 75.59, H% 8.03.

Synthesis of [(dippn)Ni=CHdmp][B(Ar^F)$_4$] (6). A cold (−35 °C) solution of [$FeCp_2$][BAr^F_4] (105 mg, 0.1 mmol in 5 mL of Et_2O) was added to a solution of **2** (75 mg, 0.1 mmol in 5 mL of Et_2O) at −35 °C. The mixture was stirred at ambient temperature for 30 min. After removing the volatiles under reduced pressure, the residue was triturated 3 times with 5 mL of *n*-pentane. Dissolving the residue in 5 mL of Et_2O and layering the solution with *n*-pentane at −35 °C induced crystallization. Subsequent filtration led to analytically pure **6** as light-pink crystals (120 mg, 74%). For **6**: ^{1}H NMR (298 K, 400.13 MHz, C_6H_6): δ 15.11 (br, $\Delta_{1/2}$ = 90 Hz, 4H), 11.58 (br, $\Delta_{1/2}$ = 100 Hz, 6H), 8.23 (br, $\Delta_{1/2}$ = 35 Hz, 7 H), 7.48 (s, 8H, $C_6H_2(CF_3)_2$), 7.31 (s, 4H, $C_6H_2(CF_3)_2$), 4.12 (br, $\Delta_{1/2}$ = 210 Hz, 12H), 1.51 (br, $\Delta_{1/2}$ = 30 Hz, 12 H), 0.32 (br, $\Delta_{1/2}$ = 40 Hz, 1H, C*H*(dmp)), −2.23 (br, $\Delta_{1/2}$ = 60 Hz, 6 H), −4.18 (br, $\Delta_{1/2}$ = 105 Hz, 12 H). μ_{eff} = 2.0 μ_B (Evans). Elemental analysis for $C_{79}H_{72}NiP_2BF_{24}$: C% 58.98; H% 4.51; found: C % 59.22, H% 4.20.

Reduction of [(dippn)Ni=CHdmp][B(Ar^F)$_4$] (6). A cold (−35 °C) suspension of KC_8 (5 mg, 0.037 mmol) in 2 mL of Et_2O was added dropwise to a solution of [(dippn)Ni=CHdmp][$B(Ar^F)_4$] (**6**, 60 mg, 0.037 mmol in 5 mL of Et_2O) at −35 °C. The mixture was stirred at room temperature for 30 min. The solution was concentrated to dryness and the black residue was suspended in 10 mL of hexanes. The black suspension was filtered through a plug of Celite. Cooling the solution at −35 °C induced the crystallization of **2**. The emerald-green crystals of (dippn)Ni=CH(dmp) (**2**, 23 mg, 0.030 mmol, 85%) were separated by decanting the mother liquor and dried under reduced pressure.

DFT Calculations. Gaussian 03 (revision D.02) was used for all reported calculations.[46] The B3LYP (DFT) method was used to carry out the geometry optimizations on the model compounds specified in text using the LANL2DZ basis set. The validity of the true minima was checked by the absence of negative frequencies in the energy Hessian. Tables with atomic coordinates of the optimized geometries can be found in the Supporting Information.

X-ray Diffraction. Data were collected on a Siemens platform goniometer with a charged coupled device (CCD) detector. Structures were solved by direct methods using the SHELXTL (version 5.1) program library (G. Sheldrick, Bruker Analytical X-ray Systems, Madison, WI).[47] All atoms were refined anisotropically and hydrogen atoms were placed in calculated positions unless specified otherwise. Tables with atomic coordinates and equivalent isotropic displacement parameters are listed in the cifsin the Supporting Information. The crystals were coated with oil (STP Oil Treatment) on a glass slide, which was brought outside the glovebox.

X-ray Crystal Structure of 3. X-ray quality crystals were obtained by slow crystallization at −35 °C from a concentrated pentanes solution. A 0.03 × 0.03 × 0.01 mm^3, dark-yellow block was chosen and mounted on the diffractometer. A total of 26091 reflections ($-11 \le h \le 11$, $-29 \le k \le 22$, $-25 \le l \le 26$) was collected at T = 100(2) K with θ_{max} = 28.26°, of which 9703 were unique (R_{int} = 0.0430). The residual peak and hole−electron density were 0.258 and −0.105 eÅ^{-3}. The least-squares refinement converged normally with residuals of R_1 = 0.0503 ($I > 2\sigma(I)$) and GOF of 1.076. Crystal and refinement data for **3**: $C_{43}H_{66}NiN_2P_2$, space group $P2_1/n$, a = 8.8867(18) Å, b = 22.452(5) Å, c = 20.673(4) Å, $\alpha = \gamma$ = 90°, β = 93.025(4)°, V = 4119.1(14) Å^3, Z = 4, μ = 0.579 mm^{-1}, F(000) = 1584, R_1 = 0.0607, wR_2 = 0.1236 (based on all data).

X-ray Crystal Structure of 1. X-ray quality crystals were obtained by slow crystallization at −35 °C from a concentrated pentanes solution. A 0.5 × 0.3 × 0.2 mm^3, emerald-green block was chosen and mounted on the diffractometer. A total of 25363 reflections ($-11 \le h \le 15$, $-15 \le k \le 15$, $-40 \le l \le 30$) was collected at T = 100(2) K with θ_{max} = 28.28°, of which 9467 were unique (R_{int} = 0.0717). The residual peak and hole−electron density were 0.204 and −0.515 eÅ^{-3}. The least-squares refinement converged normally with residuals of R_1 = 0.0574 ($I > 2\sigma(I)$) and GOF of 0.947. Crystal and refinement data for **1**: $C_{43}H_{66}NiP_2$, space group $P2_12_12_1$, a = 11.3623(16) Å, b = 11.4984(16) Å, c = 30.630(4) Å, $\alpha = \beta = \gamma$ = 90°, V = 4001.7(9) Å^3, Z = 4, μ = 0.592 mm^{-1}, F(000) = 1528, R_1 = 0.0812, wR_2 = 0.0912 (based on all data).

X-ray Crystal Structure of 4. X-ray quality crystals were obtained by slow crystallization at −35 °C from a concentrated ether solution layered with pentanes. A 0.1 × 0.08 × 0.05 mm^3, yellow block was chosen and mounted on the diffractometer. A total of 33275 reflections ($-14 \le h \le 14$, $-17 \le k \le 17$, $-47 \le l \le 47$) was collected at T = 100(2) K with θ_{max} = 25.00°, of which 12721 were unique (R_{int} = 0.0638). The residual peak and hole−electron density were 0.685 and −0.423 eÅ^{-3}. The least-squares refinement converged normally with residuals of R_1 = 0.0504 ($I > 2\sigma(I)$) and GOF of 0.915. Crystal and refinement data for **4**: $C_{75}H_{78}BF_{24}NiP_2$, space group $P2_1/n$, a = 12.7248(17) Å, b = 14.8784(19) Å, c = 39.541(5) Å, $\alpha = \gamma$ =

dx.doi.org/10.1021/ja501900j | J. Am. Chem. Soc. 2014, 136, 6479−6488

90°, β = 93.228(3)°, V = 7474.1(17) Å^3, Z = 4, μ = 0.404 mm^{-1}, $F(000)$ = 3228, R_1 = 0.0768, wR_2 = 0.1225 (based on all data).

X-ray Crystal Structure of 5. X-ray quality crystals were obtained by slow crystallization at −35 °C from a concentrated pentanes solution. A 0.05 × 0.02 × 0.02 mm^3, dark yellow block was chosen and mounted on the diffractometer. A total of 21087 reflections ($-29 \le h \le 28$, $-24 \le k \le 20$, $-9 \le l \le 9$) was collected at T = 100(2) K with θ_{max} = 25.00°, of which 7296 were unique (R_{int} = 0.0794). The residual peak and hole−electron density were 0.932 and −0.479 eÅ^{-3}. The least-squares refinement converged normally with residuals of R_1 = 0.0593 ($I > 2\sigma(I)$) and GOF of 0.863. Crystal and refinement data for **5**: $C_{47}H_{60}N_2NiP_2$, space group $Pna2_1$, a = 24.967(4) Å, b = 20.773(3) Å, c = 8.0830(12) Å, $\alpha = \gamma$ = 90°, β = 90.907(2)°, V = 4192.1(11) Å^3, Z = 4, μ = 0.573 mm^{-1}, $F(000)$ = 1656, R_1 = 0.0593, wR_2 = 0.1231 (based on all data).

X-ray Crystal Structure of 2. X-ray quality crystals were obtained by slow crystallization at −35 °C from a concentrated pentanes solution. A 0.07 × 0.05 × 0.05 mm^3, emerald-green block was chosen and mounted on the diffractometer. A total of 10647 reflections ($-13 \le h \le 12$, $-14 \le k \le 14$, $-15 \le l \le 19$) was collected at T = 100(2) K with θ_{max} = 25.00°, of which 6970 were unique (R_{int} = 0.0465). The residual peak and hole−electron density were 1.228 and −0.378 eÅ^{-3}. The least-squares refinement converged normally with residuals of R_1 = 0.0486 ($I > 2\sigma(I)$) and GOF of 0.907. Crystal and refinement data for **2**: $C_{47}H_{60}NiP_2$, space group $P\bar{1}$, a = 14.2589(12) Å, b = 13.0889(11) Å, c = 39.706(3) Å, β = 90.907(2)°, V = 7409.5(11) Å^3, Z = 4, μ = 0.408 mm^{-1}, $F(000)$ = 3228, R_1 = 0.0775, wR_2 = 0.1433 (based on all data).

■ ASSOCIATED CONTENT

Ⓢ Supporting Information

Experimental details for compound characterizations, DFT calculation details, full crystallographic descriptions (as cif), and complete reference 46. This material is available free of charge via the Internet at http://pubs.acs.org.

■ AUTHOR INFORMATION

Corresponding Author

*E-mail: viluc@nd.edu

Present Address

Vlad M. Iluc, Department of Chemistry and Biochemistry, University of Notre Dame, Notre Dame, IN 46556.

Notes

The authors declare no competing financial interest.

Gregory L. Hillhouse was deceased March 6, 2014.

■ ACKNOWLEDGMENTS

The authors thank Marisa Monreal (UCLA) for help with EPR and SQUID measurements. This work was supported by the National Science Foundation through grants CHE-1266281 and CHE-0957816 (to G.L.H.), and CHE-1048528 (CRIF MU instrumentation). Dedicated to the memory of Gregory L. Hillhouse.

■ REFERENCES

(1) Curley, J. J.; Kitiachvilli, K. D.; Waterman, R.; Hillhouse, G. L. *Organometallics* **2009**, *28*, 2568.

(2) Waterman, R.; Hillhouse, G. L. *J. Am. Chem. Soc.* **2003**, *125*, 13350.

(3) Mindiola, D. J.; Hillhouse, G. L. *J. Am. Chem. Soc.* **2002**, *124*, 9976.

(4) Gutsulyak, D. V.; Piers, W. E.; Borau-Garcia, J.; Parvez, M. *J. Am. Chem. Soc.* **2013**, *135* (32), 11776.

(5) Mankad, N. P.; Peters, J. C. *Chem. Commun.* **2008**, *9*, 1061.

(6) (a) Dai, X.; Warren, T. H. *J. Am. Chem. Soc.* **2004**, *126*, 10085. (b) Badiei, Y. M.; Warren, T. H. *J. Organomet. Chem.* **2005**, *690*, 5989.

(7) Hamaker, C. G.; Mirafzal, G. A.; Woo, L. K. *Organometallics* **2001**, *20*, 5171.

(8) Li, Y.; Huang, J.-S.; Zhou, Z.-Y.; Ch, C.-M.; You, X.-Z. *J. Am. Chem. Soc.* **2002**, *124*, 13185.

(9) Mindiola, D. J.; Hillhouse, G. L. *J. Am. Chem. Soc.* **2001**, *123*, 4623.

(10) Melenkivitz, R.; Mindiola, D. J.; Hillhouse, G. L. *J. Am. Chem. Soc.* **2002**, *124*, 3846.

(11) An example of monodentate coordination mode for dtbpe: (κ^1-dtbpe)NiCl{N,O-η^2-TEMPO} in Mindiola, D. J.; Waterman, R.; Jenkins, D. M.; Hillhouse, G. L. *Inorg. Chim. Acta* **2003**, *345*, 299.

(12) Iluc, V. M.; Laskowski, C. A.; Hillhouse, G. L. *Organometallics* **2009**, *28*, 6135.

(13) Kawano, M.; Hirai, K.; Tomioka, H.; Ohashi, Y. *J. Am. Chem. Soc.* **2007**, *129*, 2383.

(14) Ouihia, A.; René, L.; Guilhem, J.; Pascard, C.; Badet, B. *J. Org. Chem.* **1992**, *58*, 1641.

(15) Casarrubios, L.; Perez, J. A.; Brookhart, M.; Templeton, J. L. *J. Org. Chem.* **1996**, *61*, 8358.

(16) Xie, W. H.; Fang, J. W.; Li, J.; Wang, P. G. *Tetrahedron* **1999**, *55*, 12929.

(17) Wada, S.; Shimomura, M.; Kikuchi, Y.; Yuge, H.; Miyamoto, T. K. *J. Porphyrins Phthalocyanines* **2008**, *12*, 35.

(18) Chisholm, M. H.; Heppert, J. A.; Huffman, J. C.; Ontiveros, C. D. *Organometallics* **1989**, *8*, 976.

(19) Schrock, R. R. *Chem. Rev.* **2002**, *102*, 145.

(20) Basuli, F.; Bailey, B. C.; Tomaszewski, J.; Huffman, J. C.; Mindiola, D. J. *J. Am. Chem. Soc.* **2003**, *125*, 6052.

(21) Mahias, V.; Cron, S.; Toupet, L.; Lapinte, C. *Organometallics* **1996**, *15*, 5399.

(22) Baumann, R.; Stumpf, R.; Davis, W. M.; Liang, L.-C.; Schrock, R. R. *J. Am. Chem. Soc.* **1999**, *121*, 7822.

(23) vanderHeijden, H.; Hessen, B. *J. Chem. Soc., Chem. Commun.* **1995**, 145.

(24) Liu, X. X.; Li, L.; Diminnie, J. B.; Yap, G. P. A.; Rheingold, A. L.; Xue, Z. *Organometallics* **1998**, *17*, 4597.

(25) Sur, S. K. *J. Magn. Reson.* **1989**, *82*, 169.

(26) Evans, D. F. *J. Chem. Soc.* **1959**, 2003.

(27) Kitiachvili, K. D.; Mindiola, D. J.; Hillhouse, G. L. *J. Am. Chem. Soc.* **2004**, *126*, 10554.

(28) Eaborn, C.; Hill, M. S.; Hitchcock, P. B.; Smith, D. J. *J. Chem. Soc., Chem. Commun.* **2000**, 691.

(29) Kaska, W. C.; Starzewski, K. A. *Ylides and Imines of Phosphorus*; Johnson, A. W., Ed.; John Wiley & Sons: New York, 1993; Chapter 14.

(30) Vicente, J.; Chicote, M. T. *Coord. Chem. Rev.* **1999**, *193−195*, 1143.

(31) Kolodiazhnyi, O. I. *Tetrahedron* **1996**, *52*, 1855.

(32) Falvello, L. R.; Ginés, J. C.; Carbó, J. J.; Lledós, A.; Navarro, R.; Soler, T.; Urriolabeitia, E. P. *Inorg. Chem.* **2006**, *45*, 6803.

(33) Altwicker, E. R. *Chem. Rev.* **1967**, *67*, 475.

(34) Hicks, R. G. *Org. Biomol. Chem.* **2007**, *5*, 1321.

(35) Manner, V. W.; Markle, T. F.; Freudenthal, J.; Roth, J. P.; Mayer, J. M. *Chem. Commun.* **2008**, *2*, 256.

(36) Iluc, V. M.; Hillhouse, G. L. *J. Am. Chem. Soc.* **2010**, *132* (43), 15148.

(37) Blanksby, S. J.; Ellison, G. B. *Acc. Chem. Res.* **2003**, *36*, 255.

(38) Iluc, V. M.; Laskowski, C. A.; Brozek, C. K.; Harrold, N. D.; Hillhouse, G. L. *Inorg. Chem.* **2010**, *49* (15), 6817.

(39) Iluc, V. M.; Miller, A. J. M.; Anderson, J. S.; Monreal, M. J.; Mehn, M. P.; Hillhouse, G. L. *J. Am. Chem. Soc.* **2011**, *133* (33), 13055.

(40) Carlin, R. L.; van Duyneveldt, A. In *J. Magnetic Properties of Transition Metal Compounds*; Springer: Berlin, 1977.

(41) For a general description of the equipment and techniques, see: Burger, B. J.; Bercaw, J. E. In *Experimental Organometallic Chemistry*; Wayda, A. L., Darensbourg, M. Y., Eds.; ACS Symposium Series 357; American Chemical Society: Washington, DC, 1987; pp 79−98.

(42) Pangborn, A. B.; Giardello, M. A.; Grubbs, R. H.; Rosen, R. K.; Timmers, F. J. *Organometallics* **1996**, *15*, 1518.

(43) Schwindt, M. A.; Lejon, T.; Hegedus, L. S. *Organometallics* **1990**, *9*, 2814.
(44) Chavez, I.; Alvarez-Carena, A.; Molins, E.; Roig, A.; Maniukiewicz, W.; Arancibia, A.; Arancibia, V.; Brand, H.; Manriquez, J. M. *J. Organomet. Chem.* **2000**, *601*, 126.
(45) Bach, I.; Porschke, K.; Goddard, R.; Kopiske, C.; Kruger, C.; Rufinska, A.; Seevogel, K. *Organometallics* **1996**, *15*, 4959.
(46) Frisch, M. J.; et al. *Gaussian 03*, revision D.02; Gaussian, Inc.: Wallingford CT, 2004.
(47) All software and sources of scattering factors are contained in the SHELXTL (version 5.1) program library (Sheldrick, G., Bruker Analytical X-ray Systems: Madison, WI).